



EFFICIENT SIMULATION FOR OPTIMIZATION OF TOPOLOGY, SHAPE AND SIZE OF MODULAR TRUSS STRUCTURES

A. Ahrari^a and A. A. Atai^{*,†,b}

^a*Department of Mechanical Engineering, Michigan State University, East Lansing, MI, USA*

^b*School of Mechanical Engineering, College of Engineering, University of Tehran, Tehran, Iran*

ABSTRACT

The prevalent strategy in the topology optimization phase is to select a subset of members existing in an excessively connected truss, called Ground Structure, such that the overall weight or cost is minimized. Although finding a good topology significantly reduces the overall cost, excessive growth of the size of topology space combined with existence of varied types of design variables challenges applicability of evolutionary algorithms tailored for simultaneous optimization of topology, shape and size (TSS) in more complicated cases which are of great practical interest. In practice, large-scale truss structures are often modular, formed by joining periodically repeated units. This article organizes a novel simulation approach for this class of truss structures where the main drawbacks of the ground structure-based simulation approach are greatly moderated. The two approaches are independently employed for simultaneous TSS optimization of a modular truss example and the size of topology space as well as the required computation budget to generate an acceptable candidate design is compared. Result comparison reveals by employing the novel approach, problem complexity grows linearly with respect to the number of modules which allows for expanding application of TSS optimizers to complex modular trusses. Use of relative coordinates is also warranted for shape optimization which concludes to a more efficient optimization process.

Received: 10 December 2012; Accepted: 5 March 2013

KEY WORDS: truss optimization; topology space; sampling complexity; ground structure; relative coordinates

* Corresponding author: A. Atai, School of Mechanical Engineering, College of Engineering, University of Tehran, Tehran, Iran

†E-mail address: aataee@ut.ac.ir (A. A. Atai)

1. INTRODUCTION

Truss optimization can be performed at three distinct levels: Specifying the optimal cross sections of members (size optimization), coordinates of nodes (shape or configuration optimization) or the existing nodes and their connection plot (Topology optimization) [1].

The common strategy in topology optimization phase is to select a subset of members existing in an excessively connected truss, called “Ground Structure” [2], such that the objective function is minimized. Based on loading condition and the selected ground structure, some nodes, called basic nodes [3] may not be removed. Other nodes, known as non-basic nodes, can be absent (passive) or present (active) in a candidate design. The same terminology is also used for a present or absent member. If a sample design is stable and includes all basic nodes, it will be considered acceptable, otherwise discarded or heavily penalized. Since all sampled topologies are subset of the selected ground structure, the fitness of the final design relies on reasonable configuration of this structure. Sometimes, the so-called all-to-all scheme is exploited in which all nodes in the ground structure are connected to each other. This scheme may seem preferable as it provides more topologically distinct designs, yet, it excludes any engineering knowledge on the problem at hand, resulting in excessive growth of acceptable albeit inefficient designs.

Application of meta-heuristic algorithms for truss optimization has gained much interest during the recent decade [1]. In comparison with deterministic approaches, they require a larger number of structural analyses, which is now possible regarding rapid development of computers. On the other hand, meta-heuristics perform a guided random sampling which allows in principle to explore a larger fraction of the search space than in the case of deterministic optimization [1]. They also recombine data of different individuals to guide the search. This enables handling nonlinear, multimodal and discontinuous truss problems, where deterministic approaches are prone to trap in undesirable local minima. In contrast to previous approaches that can only eliminate a member [2], meta-heuristics may reactivate a removed member or node during the optimization process.

Most previous studies on truss optimization by meta-heuristics, even those published recently, perform optimization at the size level only. For example, size optimization by Harmony Search Algorithm [4], Artificial Bee Colony [5], Big Bang–Big Crunch algorithm [6] Charged System Search [7, 8], Chaotic Imperialist Competitive Algorithm [9], Particle Swarm Optimization [10] and also some hybridized algorithms [11-14]. This also holds for the majority of truss optimizers recently reviewed by Lamberti and Pappalettere [1]. Hasançebi et al [15] compared performance of seven stochastic meta-heuristics for size optimization of truss structures and concluded Evolution Strategies (ESs) and Simulated Annealing (SA) are more reliable than other methods.

A more sophisticated scheme considers the joint effect of shape and size [16-20] or topology and size [21, 22]. Nevertheless, published papers on simultaneous topology, shape and size (TSS) optimization of truss structures, albeit the most potent and effective scheme [23], are comparatively scarce. This can be attributed to existence of varried types of design variables: Boolean, continuous and discrete variables should be reasonably employed for topology, shape and size optimization respectively [24]. Additionally, the number of design variables excessively grows for more intricate structures which challenges application of

meta-heuristic optimizers.

Genetic Algorithms (GAs) have been successfully utilized in TSS optimization of truss structures [3, 24, 25]. In addition to GAs, Ant Colony [23], Particle Swarm [26], Simulated Annealing [27] and differential Evolution [28] have shown promising results for some TSS truss optimization problems. However, some researchers believe the huge gap between intricacy of available benchmarks and practical problems highly limits applicability of such algorithms in practice [29]. For the simplest scenario, size optimization, intricate test problems consisting of hundreds or even thousands of members are available in the literature [11, 15, 30] which may fairly simulate complicated practical cases. However, for the most effective scenario, simultaneous TSS optimization, this challenge is conspicuously visible as available benchmarks are comparatively simple. For example, the 2D symmetric 39-bar problem introduced a decade ago [3] is possibly the most challenging and interesting benchmark for TSS optimization [23, 26, 28]. Regarding the rapid development of computation resources, lack of more complicated albeit practically interesting test problems is noticeable. The following reasons can account for limited applicability of TSS optimizers for more intricate structures:

i) The number of distinct topologies subset of the ground structure turns inordinately large for more complicated structures. Additionally, a slight modification in topology may lead to considerable variation in the state of constraint satisfaction, which intensifies this problem.

ii) TSS optimization typically demands simultaneous handling of three distinct types of variables. Reasonably Boolean for topology, continuous for shape and discrete for size optimization [24].

iii) Sampling a new topology relies on perturbation of current topology and checking its acceptability. If the number of members is smaller than a minimum (for example $2m-3$ for a 2D externally determinate truss where m stands for the number of members) or if the basic nodes are passive in the sampled topology, it is rejected; otherwise analyzed for stability. Checking stability, in turn, requires forming the reduced global stiffness matrix and calculating its condition number which consumes a considerable fraction of the CPU time required for a function evaluation. Nevertheless, it is rejected if unstable and a new candidate solution is sampled. For an intricate ground structure that has only a few extra members, these unsuccessful trials may consume the prominent fraction of computation budget.

In practice, large-scale truss structures are modular, which are formed by joining periodically repeated substructures, called modules [31]. Some familiar examples are truss bridge [30], power line truss [16], skeletal wind turbine tower [32] or horizontal jibs of tower cranes. The modules may even repeat in two directions, like in the 960-member double layer grid truss [33] or the double layer dome [34].

Modularity of the structure simplifies analysis and design of the structure. Modules can be prefabricated and assembled on site, preferably without the necessity for heavy equipment, which significantly reduces the overall cost [31]. Since the mid-1990s, however, the construction technique has changed as the computer-aided technology has advanced and custom fabrication became more efficient [31]. As a result, at times counter-intuitively, the economic advantage of modularity becomes negligible [31].

In the literature term “modularity” is generally used in a topological sense where in fact each “module” may have different geometry or requires geometrical adjustment [31]. In the present study, a more general case is considered where topology of modules may also differ to some extent. Such advanced customization, albeit increasing the computation cost, enhanced optimization efficacy and perceivably concludes to a lighter design.

Intuitively, the number of modules plays a significant role in topology optimization phase which should be specified by the optimizer, since this critical parameter is seldom known a priori. In section 3, it will be demonstrated that applicability of the ground structure method for TSS optimization of these structures, albeit possible, is inefficient even for moderate number of units, which may account for exclusion of topology optimization of these structures in previous studies and possibly in practice. This motivates introduction of computationally efficient procedures without which it could be impossible for a designer to explore all design possibilities for structures within this class. Alternatively, a new simulation method is developed, analyzed and compared to the ground structure approach from several perspectives.

2. THE BRIDGE EXAMPLE

A bridge example is investigated in this section to explore the impact of the enumerated challenges. This test problem is more complicated than most available benchmarks for shape and size optimization. The bridge, consisting of 20 equally spaced panels, is subjected to a uniformly distributed load downwards (Fig. 1a). This truss was investigated by Hasańcebi [30] to specify the optimum member areas (size) and y coordinates of upper nodes (shape). Two cases for this ground structure were studied: the Pratt model, where a single design variable is allotted for vertical position of all upper nodes and the Parker model, where vertical position of upper nodes may change independently. The extra customization introduced by the Parker model resulted in more than 38% saving in the overall weight. In this section, more customization is introduced to this problem by expanding the shape optimization phase and including an effective topology optimization phase. Impact of the enumerated factors is scrutinized when the ground structure and the unit-based structure options are employed.

2.1. Ground-structure approach

When the ground structure concept is employed, a topology optimization phase can be included by adding some extra members to the ground structure (Fig. 1b). Now the ground structure has a small degree of indeterminacy, almost equal to the number of panels. The topology optimization phase can be further expanded by enabling the algorithm to modify the number of panels. This option is of great interest since this critical parameter is seldom known a priori. Sampling a new topology in the ground structure option relies on activating a few passive or deactivating a few active members or nodes and to the author’s knowledge, only in [32] the number of units was explicitly considered as a design variable. If the ground structure option is to be employed, some extra members should be added to the ground structure so that some units could be eliminated.

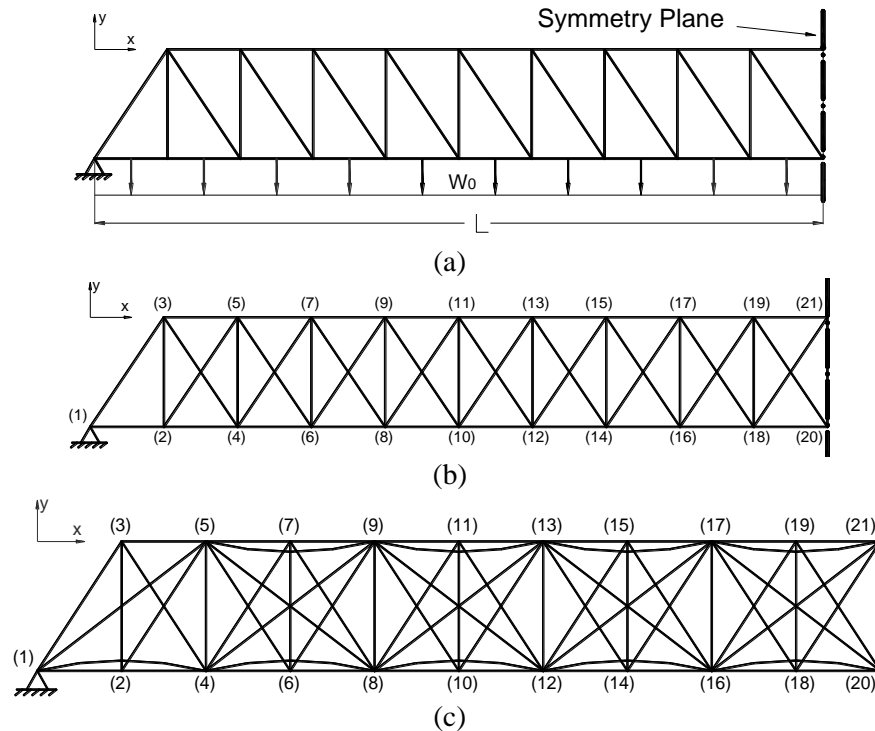


Figure 1. Optimization of truss bridge at different levels: a) A typical ground structure (half-model) for the bridge truss problem commonly used in previous studies which allows for shape and size optimization; b) Including a topology optimization phase is possible by adding a few extra members; c) Elimination of up to 5 panels is possible. For clarity, overlapping members are illustrated with curved line segments.

Figure 1c illustrates a typical instance which provides such possibilities where either of the second, fourth, sixth, eighth or tenth panel can be eliminated. Finally, the horizontal position of nodes can be modified, especially knowing that the bending moment linearly increases through the bridge span. Upper nodes may freely move along x and y directions, while for esthetic reasons, the horizontal position of lower nodes is kept identical to that of the corresponding upper nodes. This model presents a large amount of customization and as a consequence, a lighter final structure is predictable. Nevertheless, to authors' knowledge, such considerations are excluded in previous studies and possibly in practice, as the benefits of recently added options could hardly compromise with extra complexity imposed by excessive growth of topology space, even for moderate number of panels. Apart from that, including possibility of elimination of extra panels necessitates broadening the search ranges of coordinate variables pertaining to horizontal position of nodes so that distance between active nodes around a passive pair of nodes may take small values. This might lead to shapes that violate node adjacency requirement, which means for a reasonable shape, the constraints $x_{20} > x_{18} > x_{16} > \dots > x_2$ should be satisfied provided that the corresponding nodes are active. Some candidate designs may violate this requirement when the search range of x_i is enlarged. Unacceptable shapes can be discarded, but the ratio of acceptable shapes rapidly

diminishes when the number of units and the search ranges of corresponding variables are enlarged.

For truss structures, the stress limitations of the members are imposed according to the provisions of ASD-AISC [18] as follows:

2.2. Unit-based structure approach

The unit-based structure approach utilizes a different strategy to represent the problem and to generate a candidate solution which takes place in three steps. Here, these steps are explained for the bridge truss example, although this method can freely be generalized to other modular truss or even frame structures

2.2.1 Step 1: Topology

At the first step, the most distinctive parameter, the number of units or modules (K), is specified. A reasonable unit for the bridge problem is illustrated in Figure 2a which is composed of 5 members. Figure 2b illustrates the case for $K=6$. One member of each unit can be eliminated without disturbing kinematical stability of the bridge and hence, the number of acceptable substructures, called modules is $C(6,0)+C(6,1)=6$, where $C(n,k)$ means “ n choose k ” (Fig. 2c). Consequently, modules may contrast even from topological point of view, even though the basic unit is identical for all modules. The structure topology is then formed by joining these modules (Fig. 2d). In this method, modules are formed one after another, i.e. a module for the first unit is formed. If unstable, it is rejected and a new candidate module is tried. This process continues until an acceptable module is found for this unit. After that, the process of finding an acceptable module for the second unit is initiated.

2.2.2 Step 2: Shape

The shaping stage consists of determining vertical (y_i) and horizontal (x_i) positions of upper nodes. As modules are joined along x direction, relative coordinates are utilized to specify horizontal position of each node with respect to the nearest node on the left side. These relative coordinates may take any arbitrary positive value without violating node adjacency requirement. At current mode, no constraint is imposed on the overall length of the bridge.

2.2.3 Step 3: Size

Member areas are specified from the given set. This step is similar to the corresponding step in the ground structure approach. For the simple ES-based optimizer provided in the appendix, it is carried out by mutation of the size parameters of the recombinant. If the given set of available sections is discrete, the resultant value is rounded to the nearest larger value.

For evaluation purposes, shape variables corresponding horizontal positions of nodes are multiplied by a constant, α , so that the overall length of the truss becomes L (Fig. 2e).

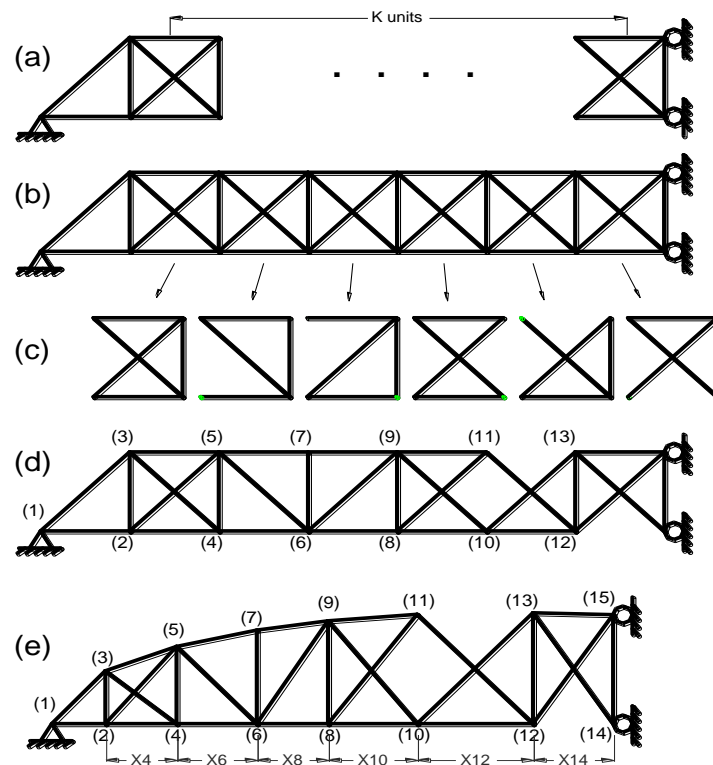


Figure 2. Steps to generate a candidate solution when the unit-based structure is employed. From top to bottom: a) The first step is to determine the number of units; b) The number of units is specified ($K=6$); c) The module pertaining to each unit is determined independently. For the selected unit, at most one member of each unit may be eliminated; d) the candidate topology is formed by joining these modules; e) shape variables are determined

3. UNIT-BASED METHOD VERSUS THE GROUND STRUCTURE APPROACH

In comparison with the conventional approach of the ground structure, the unit-based approach enjoys three principle privileges:

3.1. Size of topology space

The number of acceptable topologies that may be sampled during the optimization process is a critical factor affecting complexity of topology optimization phase. A descriptive experimentation is performed to compare this number for the bridge truss example when i) the conventional method of the ground structure and ii) the unit-based structure is employed. The objective is to determine the optimum number of panels (units) and to deactivate inefficient members. The selected ground structure for the first approach is identical to what was illustrated in Figure 1c. The overall number of topologies is 2^m where

m is the number of members in the ground structure. To calculate the number of acceptable topologies, experimental simulation is performed according to which a sufficient number of topologies subset of the ground structure is sampled where each member is considered active with a probability of 0.5. The ratio of acceptable topologies to all sampled topologies is calculated and used to estimate the overall number of acceptable topologies. When the unit-based structure is employed, 6 distinct acceptable sub-topologies (modules) can be selected for each unit and hence, the number of topologies when K units ($K+1$ panels) are selected is 6^K , and the overall number of acceptable topologies is $6^{K_{\min}} + 6^{K_{\min}+1} + \dots + 6^{K_{\max}}$.

Figure 3 illustrates the number of acceptable topologies as a function of the maximum number of panels. For either case it is assumed that the minimum number of panels is equal to half of the maximum number.

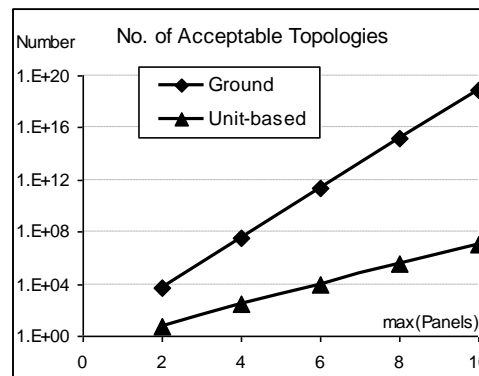


Figure3. The number of acceptable topologies as a function of the maximum number of panels when using the ground structure and the unit-based structure approaches

The plots clearly demonstrate the huge gap between the growth rates of topology space when using these approaches. When the maximum number of panels is 10, which is a moderate number, the ratio of the number of acceptable topologies when the ground structure approach is employed to this number when the unit-based structure approach is used becomes more than 6×10^{11} . The plots also demonstrate that the logarithm of the number of acceptable topologies grows linearly with respect to the maximum number of units and the gap between two plots rapidly increases.

3.2. Required effort to generate an acceptable topology

In topology optimization phase, sampling a new topology is performed by mutation and recombination of current solutions. Quite often the majority of sampled topologies are unacceptable, especially when the degree of indeterminacy of the ground structure is small. These unacceptable topologies are either discarded or severely penalized, but are not counted in function evaluations as they do not undergo FE analysis. Nevertheless, this procedure may drastically slow down optimization process since forming the reduced stiffness matrix and computing its condition number consumes a partial time of an evaluation. When the unit-based structure is employed, the stability of the candidate topology is verified by verifying some conditions in modules instead of analyzing the

stiffness matrix. The advantages of this procedure are two-fold: first, the consumed time is lessened as modules are formed independently and second, for simple base units, the acceptability of a module relies on existence of sufficient members. For the bridge problem, for instance, the candidate topology is acceptable if each module has at least 4 out of 5 members and hence, checking acceptability of the candidate topology requires neither forming the stiffness matrix nor calculating its condition number. In the first iteration, all probability mass function of all acceptable topologies should be similar. The method employed here considers each member of a unit active with a probability of 0.5 and rejects the unstable topologies.

Figure 4 illustrates the number of tried topologies and the consumed CPU time to generate an acceptable topology as a function of the maximum number of panels. Again the minimum number of panels was supposed to be equal to the half of the maximum number of panels and sampling was performed uniformly over the acceptable feasible space. For the ground structure approach, a sampled topology is first checked for having basic nodes and existence of a minimum of active members. If confirmed, it undergoes calculating the condition number of the stiffness matrix to check kinematic stability. For unstable topologies, this number is theoretically infinite, nonetheless, when it is numerically calculated, a large value may be concluded due to unavoidable rounding errors. Accordingly, large values of this number (for example larger than 10^{10}) refers to unstable topologies. The condition number of the reduced stiffness matrix is also a good measure for sensitivity of the solution to errors in input data which is of great importance when robust optimization is desired.

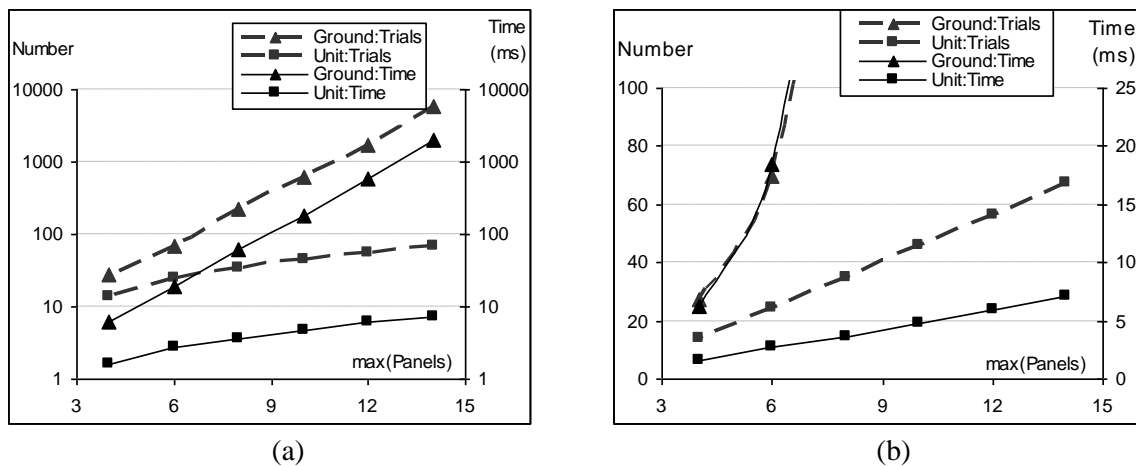


Figure4. Required CPU Time (ms) and the number of tried topologies to generate an acceptable topology as a function of maximum number of units when the concepts of the ground structure (GS) and the Unit-based structure (UBS) are employed: a) logarithmic scale; b) linear scale.

The test was run on a 4-core processor (4×2.66 GHz) PC with 2G RAM. The plots demonstrate that both the number of tried topologies and the required computation time grow exponentially when the ground structure approach is employed while they grow

linearly when the unit-based structure is employed. When the maximum number of panels is selected as 14, the required time to generate an acceptable topology becomes more than 1 second, which implies that application of the ground structure approach is impractical. If the unit-base structure is employed, the corresponding time is only 7 ms.

3.3. Size of topology space

As relative coordinates is employed, the range of shape variables can be set to $(0, u_0]$ while the requirement for nodal adjacency is always fulfilled and adjacent nodes may approach as close as desired. Apart from that, knowing that variation in height of the bridge would be gradual, use of relative coordinates even for vertical position of the upper nodes could be beneficial. To check this experimentally, the bridge example is optimized for shape and size while its topology is similar to what was presented in Figure 1a.

Table 1. Data for simulation of the bridge truss problem

Design Variables	
Shape (19)	$x_3, y_3, x_5, y_5, x_7, y_7, x_9, y_9, x_{11}, y_{11}, x_{13}, y_{13}, x_{15}, y_{15}, x_{17}, y_{17}, x_{19}, y_{19}, y_{21}$
Size (48)	$a_i, i=1,2,\dots,48$
Constraints	
Stress	$(\sigma_c)_i \leq 36$ (248.2 MPa) ksi ; $(\sigma_t)_i \leq 36$ ksi (248.2 MPa), $i=1,2,\dots,48$
Displacement	$u_i \leq 10$ in (25.4 cm)
Buckling	$ (\sigma_c)_i \leq \alpha E a_i / l_i^2, i=1,2,\dots,48, \alpha=4$
Search Range	
Shape Variables	Absolute
	$150(i-1)-200 \leq x_i \text{ in} \leq 150(i-1)+200, i=3,5,\dots,19$
	$381(i-1)-508 \leq x_i \text{ cm} \leq 381(i-1)-508, i=3,5,\dots,19$
	$50 \text{ in} (127 \text{ cm}) \leq y_3 \leq 1000 (2540 \text{ cm})$
	$50 \text{ in} (127 \text{ cm}) \leq y_i \leq 1500 \text{ in} (3810 \text{ cm}), i=3,5,\dots,21$
	$100 \leq x_i \leq 900, i=3,5,\dots,19$
Relative	
$50 \text{ in} (127 \text{ cm}) \leq y_3 \leq 1000 \text{ in} (2540 \text{ cm});$	
$-100 \text{ in} (-254 \text{ cm}) \leq y_i \leq 300 \text{ in} (762 \text{ cm}), i=5,7,\dots,21$	
Size Variables	$1 \text{ in}^2 (6.45 \text{ cm}^2) \leq A_i \leq 100 \text{ in}^2 (645.15 \text{ cm}^2)$
Loading	
$W=-200 \text{ lb/in} (-35025 \text{ N/m})$	
Mechanical Properties	
Modulus of elasticity: $E=29000 \text{ ksi} (200 \text{ GPa})$	
Density of the material: $\rho=0.3 \text{ lb/in}^3 (0.0814 \text{ N/cm}^3)$	

Shape optimization includes determining vertical and horizontal position of upper nodes by a simple ES-based optimizer explained in appendix. The following options for representation of nodal coordinates are employed independently:

- I) Absolute coordinates for both vertical and horizontal position of the nodes.

- II) Absolute coordinates for vertical but relative coordinates for horizontal position of the nodes.
- III) Relative coordinates for both vertical and horizontal position of the nodes.

If relative coordinates are used, the design variable specifies vertical/horizontal distance from the node on the left side in the same cord. Data required for simulation is presented in Table 1. For each case 50 independent runs were executed while population size and maximum number of iterations were set to 200 and 1000 respectively. Having analyzed output data, Expected Running Time (ERT) to reach a target structural weight was computed according to the following relation [35]:

$$ERT = FE_S / SR \tag{1}$$

where SR denotes the fraction of runs that could reach the desired target weight and FE_S is the average number of evaluations of successful runs to reach that weight. The calculated values of ERT as a function of the target weight are plotted in Figure 5a. Figure 5b depicts the best solution found by each option and corresponding data is presented in Table 2.

Table 2 Best solution found in case I, case II and case III. Coordinates and areas are presented in ft and in² respectively

Variable	Case I	Case II	Case III	Variable	Case I	Case II	Case III	Variable	Case I	Case II	Case III
x_3	19.45	4.92	6.61	a_{1-3}	30.518	30.281	44.379	a_{11-13}	42.357	39.366	33.640
y_3	18.22	6.18	8.07	a_{2-3}	1.402	1.003	1.003	a_{12-13}	1.094	1.000	1.000
x_5	42.06	9.83	14.87	a_{2-4}	29.057	38.524	27.082	a_{12-14}	38.904	30.876	18.778
y_5	28.54	9.65	15.47	a_{3-4}	8.897	28.145	10.232	a_{13-14}	4.217	3.593	1.578
x_7	67.67	17.00	28.64	a_{3-5}	34.204	38.566	31.815	a_{13-15}	58.248	38.467	31.834
y_7	42.42	14.74	25.82	a_{4-5}	18.537	33.624	3.716	a_{14-15}	1.000	1.023	1.709
x_9	88.54	30.75	47.46	a_{4-6}	26.826	20.590	15.556	a_{14-16}	35.036	29.030	19.073
y_9	51.95	24.44	40.36	a_{5-6}	1.821	10.810	2.844	a_{15-16}	1.342	2.517	1.202
x_{11}	121.38	60.50	70.88	a_{5-7}	38.557	42.746	21.812	a_{15-17}	38.354	40.998	40.983
y_{11}	63.95	42.08	55.70	a_{6-7}	1.000	7.055	5.521	a_{16-17}	1.715	2.030	2.350
x_{13}	145.90	94.17	101.44	a_{6-8}	33.448	25.297	19.435	a_{16-18}	38.214	31.734	19.382
y_{13}	71.08	57.78	71.80	a_{7-8}	2.276	4.464	1.002	a_{17-18}	1.784	3.926	1.332
x_{15}	168.75	129.17	131.77	a_{7-9}	33.841	28.783	23.805	a_{17-19}	34.333	42.499	35.470
y_{15}	75.97	69.56	84.96	a_{8-9}	1.000	1.001	1.000	a_{18-19}	1.332	1.615	2.290
x_{17}	196.41	167.50	171.75	a_{8-10}	30.887	22.436	17.959	a_{18-20}	40.126	32.652	20.816
y_{17}	80.60	79.71	98.17	a_{9-10}	2.976	2.970	1.314	a_{19-20}	1.003	1.737	1.000
x_{19}	222.81	207.50	209.04	a_{9-11}	38.333	36.183	27.613	a_{19-21}	42.107	44.034	38.449
y_{19}	82.43	84.34	104.33	a_{10-11}	1.000	1.000	1.000	a_{20-21}	1.000	1.000	1.000
x_{21}	82.90	85.28	105.96	a_{10-12}	34.449	23.556	18.208	Weight			
a_{1-2}	23.022	28.507	28.487	a_{11-12}	2.769	3.147	1.871	(lb)	77219	73818	58457

5. SUMMARY AND CONCLUSIONS

The huge gap between complexity of the test and practical problems for simultaneous optimization of topology, shape and size (TSS) challenges applicability of truss optimizers in more complicated situations. In practice, modular trusses are frequently observed in which a multitude of detectable yet simple modules comprise the main truss. This study provides a novel approach, called the unit-based methods, for simulation of this class of truss structures. To compare this method with the prevalent method of the ground structure, a truss bridge consisting of several panels was scrutinized. A reasonable ground structure

which allowed for generating candidate solutions with different number of panels was configured. It was demonstrated that the required computation effort, measured in the forms of the number of unacceptable sampled candidates and CPU time to generate an acceptable topology, when the ground structure option is employed, grows exponentially with respect to the number of panels which restrict applicability of this option even for moderate number of panels. On the contrary, these quantities grow linearly when the unit-based method is employed and besides, the size of topology space grows at much lower rate in comparison with the ground structure approach. Apart from that, use of relative coordinates was strongly advocated by empirical results from a simple ES-based optimizer. Comparison among plots of ERT and quality of the final solution confirmed benefits of relative coordinates for both horizontal and vertical nodal positions.

The unit-based method can be employed by meta-heuristics to handle the problem complexity of TSS optimization for larger structures. This, in fact, can reduce the gap between the intricacy of truss structures in practice and those employed as benchmarks in literature. More complex test functions, within fixed computation resources, can compare applicability and practicality of truss optimizers more reliability, which is a step forward to extend application of stochastic optimization algorithms in engineering.

REFERENCES

1. Lamberti L, Pappalettere C. Metaheuristic design optimization of skeletal structures: a review, *Comput Technol Reviews*, 2011; **4**: 1–32.
2. Topping BHV. Shape optimization of skeletal structures: a review, *J Struct Eng, ASCE* 1983; **109**(8): 1933–51.
3. Deb K, Gulati S. Design of truss-structures for minimum weight using genetic algorithms, *Finite Elem Anal Des* 2001; **37**(5): 447–65.
4. Degertekin SO. Improved harmony search algorithms for sizing optimization of truss structures, *Comput Struct* 2012; **92-93**: 229–41.
5. Sonmez M. Artificial Bee Colony algorithm for optimization of truss structures, *Appl Soft Comput*, 2011; **11**(2): 2406–2418.
6. Kaveh A, Talatahari S. Size optimization of space trusses using Big Bang–Big Crunch algorithm, *Comput Struct* 2009; **87**(17): 1129–40.
7. Kaveh A, Talatahari S. Optimization of large-scale truss structures using modified charge system search, *Int J Optim Civil Struct Eng* 2011; **1**: 15–28.
8. Kaveh A, Talatahari S. Optimal design of skeletal structures via the charged system search algorithm, *Struct Multidiscip Optim* 2010; **41**(6): 893–911.
9. Talatahari S, Kaveh A, Sheikholeslami R. Chaotic imperialist competitive algorithm for optimum design of truss structures, *Struct Multidiscip Optim* 2012; **46**(3): 355–67.
10. Li LJ, Huang ZB, Liu F, Wu QH. A heuristic particle swarm optimizer for optimization of pin connected structures, *Comput Struct* 2007; **85**(7): 340–49.
11. Rahami H, Kaveh A, Aslani M, Najjan-Asl R. A hybrid modified Genetic-Nelder Mead Simplex algorithm for large-scale truss optimization, *Int J Optim Civil Struct Eng* 2011; **1**: 29–46.

12. Kaveh, A. and S. Talatahari, Particle swarm optimizer, ant colony strategy and harmony search scheme hybridized for optimization of truss structures, *Comput Struct* 2009; **87**(5): 267–83.
13. Hadidi A, Kaveh A, Farahmand-Azar B, Talatahari S, Farahmandpour C. An efficient hybrid algorithm based on particle swarm and simulated annealing for optimal design of space trusses, *Int J Optim Civil Struct Eng* 2011; **1**(3): 377–95.
14. Kaveh A, Zolghadr A. Truss optimization with natural frequency constraints using a hybridized CSS-BBBC algorithm with trap recognition capability, *Comput Struct* 2012; **102–103**: 14–27.
15. Hasançebi O, Çarbaş S, Doğan E, Erdal F, Saka MP. Performance evaluation of metaheuristic search techniques in the optimum design of real size pin jointed structures. *Comput Struct* 2009; **87**(5): 284–302.
16. Lee KS, Han SW, Geem ZW. Discrete size and discrete-continuous configuration optimization methods for truss structures using the harmony search algorithm. *Int J Optim Civil Struct Eng* 2011; **1**: 107–26.
17. Šilih S, Kravanja S, Premrov M. Shape and discrete sizing optimization of timber trusses by considering of joint flexibility, *Adv Eng Software* 2010; **41**(2): 286–94.
18. Lamberti L, An efficient simulated annealing algorithm for design optimization of truss structures. *Comput Struct* 2008; **86**(19): 1936–53.
19. Gholizadeh S, Barzegar A, Gheytratmand C. Shape optimization of structures by modified harmony search. *Int J Optim Civil Struct Eng* 2011; **1**(3): 485–94.
20. Gholizadeh S, Barati H. A comparative study of three metaheuristics for optimum design of trusses. *Int J Optim Civil Struct Eng* 2012; **3**: 423–41.
21. Ruiyi S, Liangjin G, Zijie F. Truss Topology Optimization Using Genetic Algorithm with Individual Identification. *Proceedings of the World Congress on Engineering*, London, UK, 2009.
22. Su R, Wang X, Gui L and Fan Z. Multi-objective topology and sizing optimization of truss structures based on adaptive multi-island search strategy. *Struct Multidiscip Optim* 2011; **43**(2): 275–86.
23. Luh GC, Lin CY. Optimal design of truss structures using ant algorithm. *Struct Multidiscip Optim* 2008; **36**(4): 365–79.
24. Rajan SD. Sizing, shape, and topology design optimization of trusses using genetic algorithm, *J Struct Eng* 1995; **121**(10): 1480–7.
25. Rahami H, Kaveh A, Gholipour Y. Sizing, geometry and topology optimization of trusses via force method and genetic algorithm. *Eng Struct* 2008; **30**(9): 2360–9.
26. Luh GC, Lin CY. Optimal design of truss-structures using particle swarm optimization, *Comput Struct* 2011; **89**(23): 2221–32.
27. Hasançebi O, Erbatur F. Layout optimisation of trusses using simulated annealing. *Adv Eng Software* 2002; **33**(7): 681–96.
28. Wu CY, Tseng KY. Truss structure optimization using adaptive multi-population differential evolution, *Struct Multidisc Optim* 2010; **42**(4): 575–90.
29. Alimoradi A, Foley CM, Pezeshk S. Benchmark Problems in Structural Design and Performance Optimization: Past, Present, and Future-Part I, *In 19th Analysis and Computation Specialty Conference*, 2010.

30. Hasançebi O. Adaptive evolution strategies in structural optimization: Enhancing their computational performance with applications to large-scale structures. *Comput Struct* 2008; **86**(1): 119–32.
31. Zawidzki M, Nishinari K. Modular Truss-Z system for self-supporting skeletal free-form pedestrian networks. *Adv Eng Software* 2012; **47**(1): 147–59.
32. Noilublao N, Bureerat S. Simultaneous topology, shape and sizing optimisation of a three-dimensional slender truss tower using multiobjective evolutionary algorithms. *Comput Struct* 2011; **89**(23–24): 2531–38.
33. Kaveh A, Talatahari S. Optimization of large-scale truss structures using modified charged system search, *Int J Optim Civ Struct Eng* 2011; **1**: 15–28.
34. Kaveh A, Fazli H. Free vibration analysis of locally modified regular structures using shifted inverse iteration method. *Comput Struct* 2012; **108–109**: 75–82.
35. Auger A, Hansen N. A restart CMA evolution strategy with increasing population size. *Proceedings of the 2005 IEEE Congress on Evolutionary Computation*, 2005, pp. 1769–76.
36. Beyer H-G. Schwefel H-P. Evolution strategies—A comprehensive introduction, *Nat Comput* 2002. **1**(1): 3–52.
37. Hansen N, Ostermeier N. Completely derandomized self-adaptation in evolution strategies. *Evol Comput* 2001; **9**(2): 159–95.

APPENDIX: ES-BASED OPTIMIZER (SHAPE AND SIZE)

The employed truss optimizer is based on a standard $(\mu/\mu_w, \lambda)$ -ES for continuous optimization. For detailed information on contemporary Evolution Strategies for continuous parameter optimization the readers are referred to [36]. The following algorithmic options were used:

- $\mu = [\lambda/2]$
- An independent step size for each design (object variable) which is self-adapted.
- Simultaneous Mutation of all variables by Interrupted Normal distribution.
- Global weighted recombination for both design (object) and strategy variables.

Infeasible individuals are penalized as follows:

$$f = W \times (1 + P_s + P_b + P_d)$$

where

$$P_s = \sum_{i=1}^{N_m} (p_{si}^2 - 1), p_{si} = \begin{cases} |\sigma_i / \sigma_y^{all}| & \text{if } \sigma_{ji} > \sigma^{all} \\ 1 & \text{if else} \end{cases}, i = 1 \dots N_m$$

$$P_b = \sum_{i=1}^{N_m} (p_{bi}^2 - 1), p_{bi} = \begin{cases} \sqrt{|\sigma_i / \sigma_b^{all}|} & \text{if } (|\sigma_i| > \sigma_b^{all}) \& (\sigma_i < 0) \\ 1 & \text{if else} \end{cases}, i = 1 \dots N_m$$

$$P_d = \sum_{i=1}^{N_n} (p_{di}^2 - 1), p_{di} = \begin{cases} |d_i / d^{all}| & \text{if } \sigma_{ji} > \sigma^{all} \\ 1 & \text{if else} \end{cases}, i = 1 \dots N_n$$

The following is the pseudo code of a standard ES for unconstrained continuous

optimization. For each design variable, an independent step size is allotted which is self-adapted:

- 1: Specify λ and search ranges of design variables (\mathbf{L}, \mathbf{U})
- 2: Let $\mu = \lceil \lambda/2 \rceil$, $\tau_0 = 2(N_{\text{VAR}})^{(-0.5)}$, $\tau = 2(N_{\text{VAR}})^{(-0.25)}$, where N_{VAR} refers to the number of design variables which is equal to overall number of shape and size variables.
- 4: Sample the initial design, \mathbf{X}_R , randomly within the range. Let the initial step size vector, σ_R , be one-fourth of the corresponding search range
- 5: While not a convergence criterion is satisfied
- 6: Repeat until λ candidate solutions are generated:
- 7: Generate σ_j by mutation of σ_R according to the following relation:

$$\bar{\sigma}_j = (\exp(\tau_0 N(0,1)) \bar{\sigma}_R) \otimes [\exp(\tau N(0,1)), \exp(\tau N(0,1)), \dots, \exp(\tau N(0,1))]$$

where \otimes denotes element-wise multiplication and $N(0,1)$ refers to a random number sampled from Standard Normal distribution.
- 8: Generate \mathbf{X}_j by using σ_j as the vector of step sizes from interrupted Normal Distribution. If \mathbf{X}_j fulfills node adjacency requirement, accept it, otherwise try sampling a new candidate solution.
- 9: Calculate f_j , the objective function value at \mathbf{X}_j .
- 11: End Repeat
- 12: Sort individuals according to their fitness. Update σ_R and \mathbf{X}_R according to the following relations:

$$\bar{\mathbf{X}}_R = \sum_{k=1}^{\mu} w_k \times \bar{\mathbf{X}}_k; \sigma_R = \exp\left(\sum_{k=1}^{\mu} (w_k \times \log(\sigma_k))\right);$$

where w_k is the weight of the k^{th} parent (after sorting). Similar to the CMA-ES code, a logarithmic scale is used for the weights [37]:

$$w_k = \omega_k / \sum_{j=1}^{\mu} \omega_j, \quad \omega_k = \ln(1 + \mu) - \ln(k),$$

- 13: End while